AFSSAAE

Advances in Food Science, Sustainable Agriculture and Agroindustrial Engineering 2024, 7(3), 274-284
ISSN 2622-5921

ORIGINAL RESEARCH Open Access

Characterisation of honey using high-frequency ohmic heating based on image segmentation

Elvianto Dwi Hartono[1], Anang Lastriyanto[2], Elok Zubaidah[3], and Yusuf Hendrawan[2*]

[1] Department of Robotics and Artificial Intelligence Engineering, Faculty of Engineering, Universitas 17 Agustus 1945 Surabaya, Indonesia
[2] Department of Biosystems Engineering, Faculty of Agricultural Technology, Universitas Brawijaya, Malang, Indonesia
[3] Department of Food Science and Biotechnology, Faculty of Agricultural Technology, Universitas Brawijaya, Malang, Indonesia

KEYWORDS

Heat Penetration
K-means Clustering
Ohmic Heating
Segmentation

ABSTRACT

In the field of computer vision, image segmentation using a clustering approach was employed. This non-destructive method was applied to process ohmic heating in honey, aiming to achieve an efficient and time-saving mass production process. The K-means clustering algorithm converted RGB color data to Lab color space for effective segmentation. The validation of outcomes was conducted through the evolution of RMSE values and regression analysis for each frequency. Notably, at a precision frequency of 1 kHz, the results were as follows: RMSE Red 1.4902, RMSE Green 0.7017, RMSE Blue 0.3328, Regression Red 0.0792, Regression Green 0.5782, Regression Blue 0.202, and heat penetration regression 0.658. This proposed method was benchmarked against the conventional heat penetration analysis in ohmic heating.

Introduction

Honey's benefits for human consumption include its content of multiple vitamins, minerals, and enzymes. The vitamins found in honey include thiamin (B1), riboflavin (B2), ascorbic acid (C), pyridoxine (B6), niacin, pantothenic acid, biotin, folic acid, and vitamin K. Diastase, invertase, glucose oxidase, peroxidase, and lipase are the enzymes present. Honey also contains antioxidants from enzymatic substances (catalase, glucose oxidase, and peroxidase) and non-enzymatic substances (ascorbic acid, \(\alpha\)-tocopherol, carotenoids, amino acids, proteins, Maillard reaction products, flavonoids, and phenolic acids). Instabilities in honey-containing water are influenced by various factors such as humidity, production process, honey type, and storage conditions (Alkanan et al., 2021; Makroo et al., 2020; Shafiee et al., 2014).

The development of food processing technology is now shifting towards non-thermal and non-destructive methods like ohmic heating. Ohmic heating is based on Ohm's Law, where voltage and current are applied directly to a conductor, resulting in resistance and heat generation. This method offers a more uniform heating process, preserving foods like honey's quality and nutritional value.

Ohmic heating relies on volumetric heating, necessitates high performance, and transforms electrical power into thermal energy. Its application in food processing has largely supplanted traditional pasteurization methods. This technique involves a connection between solid-state and liquid-state conductors to an alternating current source, a process driven by the Joule effect (Park et al. 2013). The conductor plays a crucial role in ensuring the current spreads more uniformly. Nonetheless, ohmic heating at low frequencies (50–60 Hz) presents challenges, such as inadequate heat penetration during the heating cycle. The ohmic heating system induces ion collisions as the ions, subjected to an electric field, migrate towards the electrode of opposite charge. This movement, prompted by the alternating current, results in ion collisions that create resistance and elevate kinetic energy. The generated heat quantity is contingent upon the food product's current, voltage, electric field strength, and electrical conductivity (Alkanan et al. 2021). Image analysis is acknowledged as a rapid, cost-effective, and non-destructive technique for assessing the quality of food products (Patrício and

*Corresponding author
E-mail address: yusuf_h@ub.ac.id

Received on 26 July 2024, Revised on 25 September 2024, Accepted on 30 September 2024

Rieder, 2018; Vithu and Moses, 2016). The adoption of computer vision for the evaluation of agricultural and food commodities has faced numerous obstacles, underscoring the necessity for a method that is both precise and swift, as well as unbiased, to evaluate the quality of the materials under scrutiny (Patel et al., 2012).

This method facilitates the creation of automated equipment for the food and agricultural industries. Numerous studies have demonstrated that K-means clustering yields optimal results in computer vision applications. The development of computer vision, aimed at inspecting the quality of food and agricultural products, has encountered several challenges. These challenges necessitate an efficient, precise, rapid, and objective approach to determining the evaluated materials' quality (Patel et al., 2012; Hendrawan and Al-Riza, 2016; Sofu et al., 2016). Clustering modeling, involving segmentation with RGB color conversion to L*a*b* and the generation of binary 1 and 0 values, allows for the differentiation of clusters within an image (Hendrawan and Al-Riza, 2016; Hendrawan and Murase, 2011b, 2011a; Sofu et al., 2016). The present study analyzed honey image data obtained from pasteurization processes using ohmic heating with aluminum electrodes at frequencies of 50 Hz, 300 Hz, 1 kHz, and 3 kHz.

Research Methods

Material

Honey, a natural sweetener produced by Apis species bees from floral nectar or other plant parts, is the focus of this study, which utilizes various Indonesian Trigona sp honey (Evahelda et al., 2021). The ohmic heating test on Trigona sp honey, harvested from coconut and palm flower nectar, involved a pasteurization process reaching 63°C with a holding time of 30 minutes at treatment frequencies of 50Hz, 300Hz, 1kHz, and 3kHz. The voltage gradient applied was 60 V/cm with an alternating current of 300 VAC.

Experimental procedure

Image acquisition was segmented into sub-units: light excitation, image capture, and sample positioning. Light excitation comprised four 50-watt halogen LED lamps connected to a power source, angled at 45° towards the object for RGB color image acquisition, positioned 150mm from the sample field unit. To mitigate halation, four CPL filters (KNF Concept) were placed in front of the LEDs, and one CPL filter plus a variable ND fader (KNF Concept) was positioned in front of the camera. Additionally, two UV LEDs (HPL 3Watt) at 395nm wavelength were arranged in a ring to capture images set 190 mm from the sample area. A UV filter between the camera and UV light allowed 0.3% light transmission at 395 nm, ensuring primary reflection phenomena. High-resolution images in RGB were captured using a Canon EOS 1500D camera, housed within a black box with a black background, as depicted in Figure 1. Image dataset processing was conducted on a 64-bit CPU computer with an AMD RYZEN 3 processor using Matlab R2018b, converting images from RGB to L*a*b* color space (Philipp and Rath, 2002). Image segmentation constructed two-part clusters for foam and honey detection, extracting each RGB component for centroid clustering. Threshold values for each RGB component were calculated, resulting in segmented clustering. Validation of RGB components was based on Root Mean Square Error (RMSE) and regression R^2.

Parameter analysis

The analysis employed RGB color conversion to L*, a*, b* and segmentation processes to form clusters represented as two-class binaries, 1 and 0, facilitating the detection of evaporation heat. Additionally, RGB colors and clustering centroids were utilized to determine the pixel value points for each threshold in red, green, and blue and for measuring clustering in each image, reflecting the K-means method's segmentation techniques. Consequently, the validation of this work is proposed using the mean Root Mean Square Error (MRMSE) for red, green, and blue, respectively.

- *Proposed algorithm*

The methodology implemented in this study encompasses the following steps: (1) utilization of a black background pixel, (2) conversion of RGB to L*a*b* color space for color partitioning, (3) partitioning into two classes for clustering, (4) image segmentation to detect foam and honey during ohmic heating using K-means clustering, (5) dimensionality reduction through thresholding to derive values, and (6) application of the input image back to RGB color space for clustering. These procedures are elaborated upon herein. Image capture was conducted at treatment frequencies of 50Hz, 300Hz, 1kHz, and 3kHz against a black background to enhance clustering accuracy and optimize processing time for ohmic heating, aiming for two-class clustering within the images.

For the Black Background Pixel step, the background is eliminated and replaced with a black

pixel to mitigate potential biases in property extraction from the input image and the clustering model. Background removal is achieved by independently normalizing the RGB color channel values. To augment usability, this task incorporates binary thresholding and pixel clustering detection for images under fundamental and natural conditions (Kumar and Tiwari, 2019).

Image segmentation is a pivotal technique in image analysis, involving the partitioning of an image into distinct regions. This process ranges from basic thresholding techniques to advanced methods in color and frequency-domain segmentation. Among these, the K-means clustering algorithm stands out as a reliable method for image thresholding due to its straightforward computational process (Bhanu and Peng, 2000; Kumar and Tiwari, 2019; Singh and Misra, 2017).

K-means clustering is a classification algorithm that organizes objects into 'K' distinct classes based on their attributes. It minimizes the sum of squared distances between objects and their respective cluster centroids. The K-means algorithm operates through the following steps: (1) initial random selection of 'K' cluster centers; (2) assignment of each pixel to the nearest cluster center; (3) recalculation of cluster centers by averaging the pixels within each cluster; and (4) repetition of steps 2 and 3 until convergence (Kaur and Kaur, 2018). The choice of 'K' and the initial cluster centers is crucial, as incorrect selection can lead to suboptimal clustering. In this context, clustering is particularly beneficial for analyzing honey's response to ohmic heating by identifying areas within the chamber tool. The study utilized K-means clustering to differentiate between foam and honey in response to high-frequency electrical heating. Selecting the appropriate region for K-means clustering involved distinguishing between the color thresholds of foam and honey. The RGB color frequency of 1kHz was identified as the most robust for clustering and thus selected for the dataset images at frequencies of 50Hz, 300Hz, 1kHz, and 3kHz. This frequency enabled rapid processing times during the ohmic heating experiments without compromising the honey's quality. To prevent fermentation and spoilage by fungi, ohmic heating must be maintained between 63°C and 65°C; exceeding 65°C risks damaging the honey's quality. Figure 2 illustrates the preparatory steps for background separation and cluster detection.

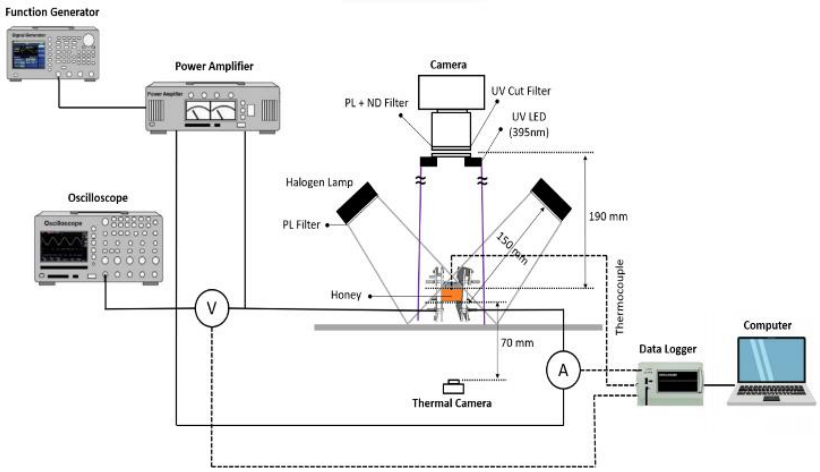

Figure 1. Imaging system component ohmic heating process

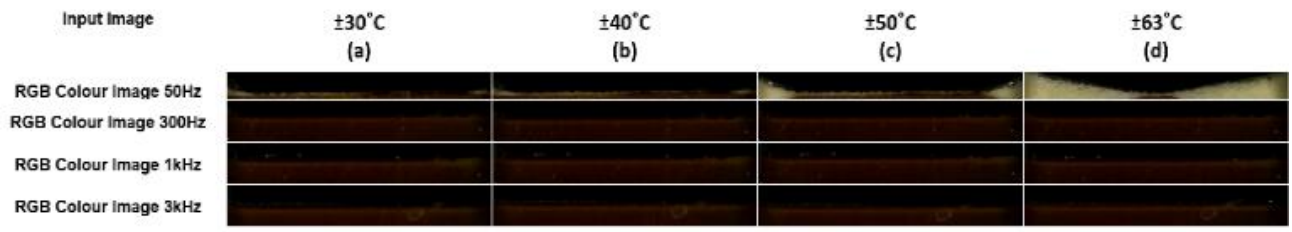

Figure 2. Honey dataset process ohmic heating: (a) Ohmic heating 30°C; (b) Ohmic heating 40°C; (c) Ohmic heating 50°C; and (d) Ohmic heating 63°C

- ***K-Means clustering algorithm***

K-means clustering is a vector quantization method from signal processing. K-means clustering aims to divide n data into K classes, where each data belongs to the nearest cluster center, as the cluster center (Dhanachandra et al., 2015; Hu et al., 2023; Javidan et al., 2023; Prakash and Singh, 2023; Xing et al., 2023). For example, given a set $X\,(x_1, x_2, \dots x_n)$, where each subset is a d-dimensional vector, to partition k-means clustering the n into $k \le n$ and set $S = (S_1, S_2, \dots S_k)$ to minimize the within-cluster Sum of Squares. Determine the center of each clustering as defined as shown in equation (1).

$$\begin{matrix} \arg\min_{S} \sum_{i=1}^{k} \sum_{x \in S_i} \|x - u_i\|^2 \\ \arg\min_{S} \sum_{i=1}^{k} |S_i| Var\,(S_i) \end{matrix} \quad \text{.....(1)}$$

Where μ defined is the mean of points in S_i. Toward the clustering calculation, μ is used as the cluster center for distance calculation optimization iterations. Minimizing the pairwise squared deviations of points in the same cluster as shown in equation (2).

$$\sum_{x,y \in S_i} \|x - u_i\|^2 = \sum_{x \ne, y \in} (x - \mu_i)^T (y - \mu_i) \text{ .(2)}$$

The K-means clustering algorithm has been widely used in engineering because it quickly and efficiently manages the local optimal. K-means clustering algorithm proposed to count a random exploration vector θ to the clustering centroid of the k algorithm as shown in equation (3).

$$D_j = D_j + \theta_j; (0 < j < k) \text{.....(3)}$$

Where θ is the random vector in d-dimensional space, obtained according to equation (4).

$$\begin{matrix} \theta_j = rand(a_i, b_i) \\ i = randsign(1,2, \dots D) \end{matrix} \quad \text{.....(4)}$$

Where the random function is a rand and sign(i) is 0 or 1. a_i and b_i are the upper and lower orders of dimension i, respectively. a_i and b_i as shown in equation (5).

$$a_i = \beta b_i \text{ .....(5)}$$

$$b_i = \alpha b_i \text{.....(6)}$$

Where β and α are a constant by the factor in the value range of [0,1], the cluster centroid tends to be stable after iterations, and the interference vector will gradually decrease. Therefore, updating the new iteration, the value of b_i changed as equation (6).

- ***Distance metrics used for clustering***

Distance metrics are pivotal in gauging the similarity among data objects. The fundamental prerequisite for metric analysis in a specific context is the procurement of a suitable distance or similarity function. Moreover, a metric or distance is a function that delineates the distance between elements or entities within a set (Singh et al., 2013). A set endowed with a metric is termed a metric space. The distance metric plays an integral role in clustering methodologies. This paper elucidates the application of the k-means clustering algorithm, employing the Euclidean distance metric. Ordinarily, the task involves defining a function of Similarity (x, y), where x and y represent disparate objects or sets of a particular class, and the function's value indicates the degree of "similarity" between the two distinct objects (Singh et al., 2013). An illustration of a generalized clustering process utilizing distance measures is depicted in Figure 3.

Similarity Measures: the distance between discrete data points can be construed as a similarity measure. Dissimilarity concerns the quantification of divergence between two data entities, while similarity denotes a value that reflects the intensity of the linkage between two data entities. The selection of an efficacious distance function for the input dataset is crucial to the success of various algorithms (Patidar et al., 2012).

Euclidean Distance: the Euclidean distance, the conventional standard for geometric problems, is fundamentally the ordinary distance between two points. It is prevalently employed in clustering challenges, particularly text clustering. The Euclidean distance is also the customary measure used by the k-means algorithm. It computes the square root of the sum of squared differences in coordinates between two entities, as demonstrated in equation (7).

$$Dist_{XY} = \max_{k} \left| X_{ik} - X_{jk} \right| \text{ ..... (7)}$$

Thresholding Algorithm: the thresholding method is split with one limit, which means the pixel values are grouped into two clusters. shown in equation (8).

$$f(x,y) = \frac{0, f_0(x,y) < 128}{255, f_1(x,y) \ge 128} \text{ ..... (8)}$$

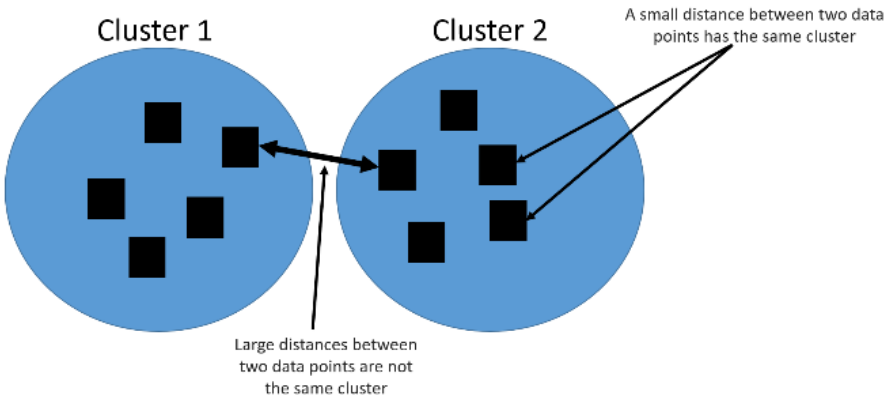

Figure 3. Illustration of the generalized clustering process using distance measures

Results and Discussion

At each heat penetration rate in the ohmic heating chamber consists of honey, acrylic, and aluminum electrodes. During the heating process at each frequency, images were captured and 37 images were obtained at each frequencies. In the experiment at the frequency of 50Hz, the average voltage input was 302.19 Vac, and the electric current was 0.114 Ampere. In contrast, the average heat penetration in honey was 24.45 Joule/s, the acrylic tube was 5.47 Joule/s and the heat penetration in the aluminum electrode was 36.90 Joule/s. Therefore, the average heat penetration in ohmic heating is 66.82 Joule/s. In the experiment at a frequency of 300Hz, the average voltage input was 303.55 Vac, and the electric current was 0.107 Ampere, while the average heat penetration in honey was 31.25 Joule/s, the acrylic tube was 6.99 Joule/s and the heat penetration in the aluminum electrode was 47.15 Joule/s. So that the average heat penetration in ohmic heating is 85.39 Joule/s. In the experiment at the frequency of 1kHz, the average voltage input was 299.86 Vac, and the electric current was 0.043 Ampere, while the average heat penetration in honey was 32.02 Joule/s, acrylic tube was 7.16 Joule/s and heat penetration in the aluminum electrode was 48.32 Joule/s. Thus, the average heat penetration in ohmic heating is 87.5 Joule/s. In the experiment at the 3kHz frequency, the average voltage input was 362.55 Vac, and the electric current was 0.052 Ampere, while the average heat penetration in honey was 29.62 Joule/s, the acrylic tube was 6.63 Joule/s and the heat penetration in the aluminum electrode was 44.69 Joule/s. So that, the average heat penetration in ohmic heating is 80.94 Joule/s.

A total of 148 color input images were captured during the ohmic heating process, with each frequency—50 Hz, 300 Hz, 1 kHz, and 3 kHz—contributing 37 images. These images are illustrated in Figure 2. Before processing, the input image dimensions for all frequencies were 270 x 40 pixels. The aim was to optimize heat penetration and efficiency in the ohmic heating process for each frequency. This study's results in computer vision segmentation clustering, applied to the honey ohmic heating process, demonstrate heat penetration at the aforementioned frequencies. The outcome of the segmentation clustering in red, green, and blue colors provides a solution in computer vision, as shown in Figure 4. Validation calculations, including RMSE RGB and regression, were performed to determine heat penetration from the experiments conducted in a chamber, as well as to enhance time efficiency and mass honey production.

Qualitative and quantitative analyses indicate that the 1 kHz frequency is more efficient than the others, requiring less time to achieve optimal heat penetration in ohmic heating. The qualitative results for the 50 Hz, 300 Hz, 1 kHz, and 3 kHz frequencies, processed through image segmentation clustering, are displayed in Figure 4. Quantitative results for each process analysis are presented in Tables 1, 2, and 3, with Table 3 showing the average quantitative result across all frequencies.

Figures 5, 6, and 7 depict the relationship between the heat penetration process in ohmic heating and the number of red values, validated by the Root Mean Square Error (RMSE) for red, green, and blue, and the regression for red, green, and blue, respectively. The computer vision solution employed in this study ensures that the computational segmentation performance at 1 kHz is stable and efficient for the heat penetration process in ohmic heating, suitable for industrial applications.

Table 1. Quantitative comparison performance in Root Means Square Error (MSE) red, green, blue, and analysis heat penetration ohmic heating validation in (A) and (B)

(a) 50Hz					(b) 300Hz				
Time/Second	**RMSE Red**	**RMSE Green**	**RMSE Blue**	**Heat Penetration OH**	**Time/Second**	**RMSE Red**	**RMSE Green**	**RMSE Blue**	**Heat Penetration OH**
0	2.3845	0.6194	0.5848	0.00	0	1.2870	0.9981	0.3362	0.00
5	2.5397	0.6723	0.6429	49.06	5	1.3369	0.8657	0.3778	68.69
10	2.1538	0.6023	0.5745	49.06	10	1.2218	0.,8994	0.2987	58.88
15	2.4381	0.6218	0.5899	49.06	15	1.2731	0.9222	0.2781	19.63
20	1.9234	0.6072	0.6145	58.88	20	1.2242	0.9174	0.2558	58.88
25	2.4769	0.6023	0.5614	58.88	25	1.1947	0.9286	0.3317	107.94
30	2.4210	0.5426	0.5145	39.25	30	1.1847	0.7654	0.2248	78.50
35	2.5595	0.6429	0.6383	68.69	35	1.2719	0.9555	0.2781	58.88
40	2.4345	0.5949	0.6023	58.88	40	1.2754	0.9755	0.2886	78.50
45	2.5850	0.4908	0.4691	58.88	45	1.1658	0.8810	0.3180	78.50
50	2.4715	0.4723	0.4847	49.06	50	1.4663	0.8306	0.2886	68.69
55	1.6140	0.4430	0.4294	68.69	55	1.2169	0.8911	0.2181	58.88
60	2.0694	0.4497	0.4397	58.88	60	1.2882	0.9010	0.3576	88.32
65	1.9203	0.4998	0.4847	58,88	65	1.2625	0.9981	0.1636	78.50
70	2.4000	0.5173	0.4878	88.32	70	1.3235	0.9831	0.2558	78.50
75	2.4624	0.5453	0.5259	58.88	75	1.2637	0.9027	0.1219	88.32
80	2.6480	0.5999	0.5949	39.25	80	1.2951	0.9238	0.3085	78.50
85	2.4038	0.5949	0.6289	78.50	85	1.2411	0.9350	0.1542	78.50
90	2.4308	0.5822	0.5848	78.50	90	1.3065	0.7635	0.1636	98.13
95	2.1511	0.5343	0.5028	39.25	95	1.2375	0.7846	0.1724	78.50
100	2.6715	0.6097	0.5561	68.69	100	1.1759	0.7673	0.1091	88.32
105	2.6965	0.6589	0,6218	58.88	105	1.2435	0.7750	0.2377	78.50
110	2.6419	0.6452	0.6313	78.50	110	1.1985	0.6962	0.1724	98,.13
115	2.5578	0.6657	0.6265	78.50	115	1.1997	0.8640	0.1443	49.06
120	2.5227	0.6475	0.6023	29.44	120	1.2684	0.6612	0.3133	98.13
125	2.6998	0.6023	0.5745	107.94	125	1.2812	0.8342	0.3317	127.57
130	2.6283	0.6383	0.5924	78.50	130	1.1772	0.7357	0.2439	98.13
135	2.5456	0.6097	0.5974	78.50	135	1.1568	0.7173	0.2314	29.44
140	0.6241	0.5398	0.5507	78.50	140	1.2719	0.8860	0.3449	157,00
145	0.5343	0.4968	0.5202	98.13	145	1.0769	0.6898	0.2499	39,25
150	0.4659	0.4562	0.4998	78.50	150	1.1229	0.8234	0.0945	147,19
155	0.4117	0.4189	0.4938	68.69	155	1.0532	0.8413	0.1542	137,38
160	0.4328	0.4659	0.4998	68.69	160	1.0797	0.7214	0.2377	117,75
165	0.4007	0.4153	0.4878	107.94	165	0.9921	0.7576	0.1091	98,13
170	0.4081	0.4259	0.4908	98.13	170	1.2625	0.6521	0.2377	127,57
175	0.4117	0.4224	0.4878	137.38	175	1.0158	0.6383	0.2558	137,38
180	0.3739	0.4044	0.4723	49.06	180	1.0560	0.4464	0.1889	127,57

Table 2. Quantitative comparison performance in root means square error (RMSE) red, green, blue, and analysis heat penetration ohmic heating validation in (C) and (D)

(c) 1kHz					(d) 3kHz				
Time/Second	**RMSE Red**	**RMSE Green**	**RMSE Blue**	**Heat Penetration OH**	**Time/Second**	**RMSE Red**	**RMSE Green**	**RMSE Blue**	**Heat Penetration OH**
0	1.4178	0.7595	0.2727	0.00	0	1.4356	1.0173	0.6657	0.00
5	1.4643	0..8143	0.3180	29.44	5	1.6204	1.0304	0.6475	39.25
10	1.4974	0.8033	0.2886	68.69	10	1.5530	1.0070	0.6429	49.06
15	1.5308	0.7921	0.2886	49.06	15	1.4418	0.9429	0.5641	58.88
20	1.4724	0.8360	0.3534	68.69	20	1.5748	0.9648	0.5999	68.69
25	1.4418	0.7214	0.3226	58.88	25	1.5405	0.9601	0.6789	58.88
30	1.4041	0.7731	0.3576	58.88	30	1.5692	0.9174	0.5641	58.88
35	1.5004	0.6723	0.2727	68.69	35	1.4469	1.0129	0.6406	78.50
40	1.4724	0.7497	0.2987	68.69	40	1.5395	0,8827	0.5426	68.69
45	1.5786	0.7537	0.2834	78.50	45	1.4147	1.1282	0.5057	58.88
50	1.4854	0.7537	0.3085	68.69	50	1.4984	0.8640	0.4627	68.69
55	1.5073	0.7276	0.2781	68.69	55	1.5004	0.9617	0.5848	68.69
60	1.3742	0.7397	0.3036	78.50	60	1.6414	0.7214	0.5641	68.69
65	1.5318	0.7214	0.3036	68.69	65	1.4387	0.7214	0.5453	68.69
70	1.6241	0.7026	0.3272	78.50	70	1.4272	0.8605	0.5561	68.69
75	1.6414	0.7316	0.3534	78.50	75	1.4561	0.7005	0.5534	78.50
80	1.4178	0.6359	0.3317	68.69	80	1.4894	0.8759	0.4878	78.50
85	1.4479	0.7357	0.3617	107.94	85	1.3402	0.7996	0.4968	68.69
90	1.4094	0.5949	0.3932	68.69	90	1.3742	0.8827	0.6194	78.50
95	1.4147	0.7255	0.3658	88.32	95	1.4924	0.8234	0.5287	98.13
100	1.4734	0.7397	0.3699	78.50	100	1.4774	0.8640	0.5507	78.50
105	1.2801	0.6745	0.2727	98.13	105	1.4052	0.7193	0.5924	98.13
110	1.3655	0.6475	0.2937	98.13	110	1.4283	0.7397	0.5899	58.88
115	1.3156	0.7276	0.3317	98.13	115	1.3402	0.8430	0.5949	88.32
120	1.4754	0.7296	0.3036	98.13	120	1.3806	0.7026	0.5057	88.32
125	1.4262	0.7110	0.3970	88.32	125	1.5201	0.7750	0.6241	186.44
130	1.4459	0.7026	0.4659	107.94	130	1.3313	0.7770	0.5614	68.69
135	1.4673	0.6941	0.3894	117.75	135	1.3313	0.6941	0.4785	19.63
140	1.4754	0.6612	0.3492	49.06	140	1.3201	0.7576	0.5231	107.94
145	1.6701	0.5873	0.2937	186.44	145	1.5318	0.7977	0.5453	88.32
150	1.4531	0.5641	0.3406	117.75	150	1.6085	0.8342	0.5693	107.94
155	1.5463	0.6723	0.3317	127.57	155	1.6940	0.7576	0.5315	98.13
160	1.7123	0.6701	0.4153	117.75	160	1.5587	0.8413	0.5588	88.32
165	1.6861	0.5480	0.2886	147.19	165	1.7010	0.6612	0.4998	117.75
170	1.5796	0.6359	0.3856	137.38	170	1.5201	0.5873	0.4723	78.50
175	1.6149	0.5899	0.3534	127.57	175	1.5122	0.7635	0.4294	137.38
180	1.5162	0.6634	0.3492	117.75	180	1.4884	0.6048	0.1091	127.57

Table 3. Quantitative average comparison performance in root means square error (RMSE) red, green, blue, and heat penetration regression ohmic heating validation. the best performances are in red, respectively.

Frequency	**RMSE Red**	**RMSE Green**	**RMSE Blue**	**Regression Red**	**Regression Green**	**Regression Blue**	**Heat Penetration Regression**
50Hz	1.6337	0.7323	0.5448	0.6313	0.0735	0.0133	0.4537
300Hz	1.5145	0.8119	0.3331	0.3121	0.531	0.2229	0.3557
1KHz	1.4902	0.7017	0.3328	0.0792	0.5782	0.202	0.658
3KHz	1.4915	0.8025	0.5056	0.0508	0.5714	0.3489	0.3557

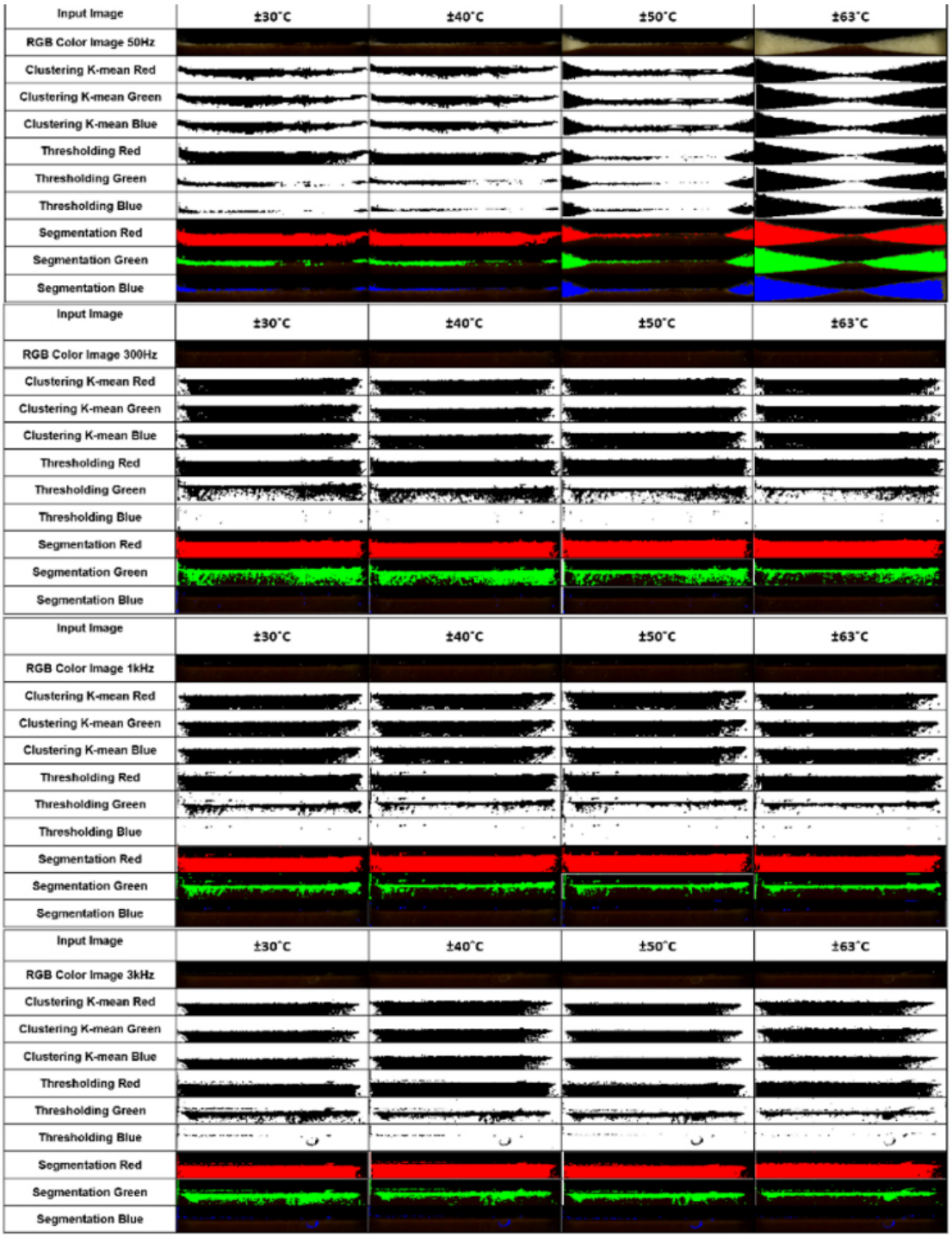

Figure 4. Qualitative result frequency 50 Hz, 300 Hz, 1 kHz, and 3 kHz image processing ohmic heating based on clustering segmentation

Figure 5. Root means square error and regression R^2 red

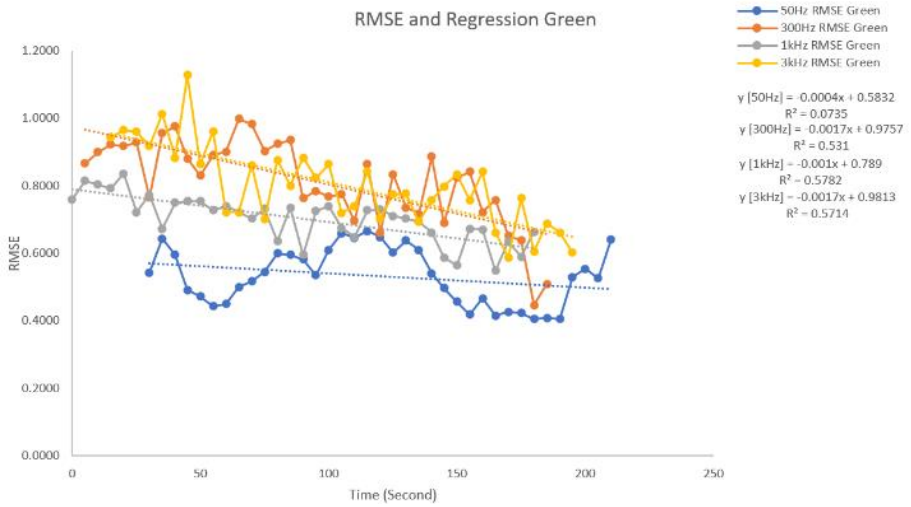

Figure 6. Root means square error and regression R^2 green

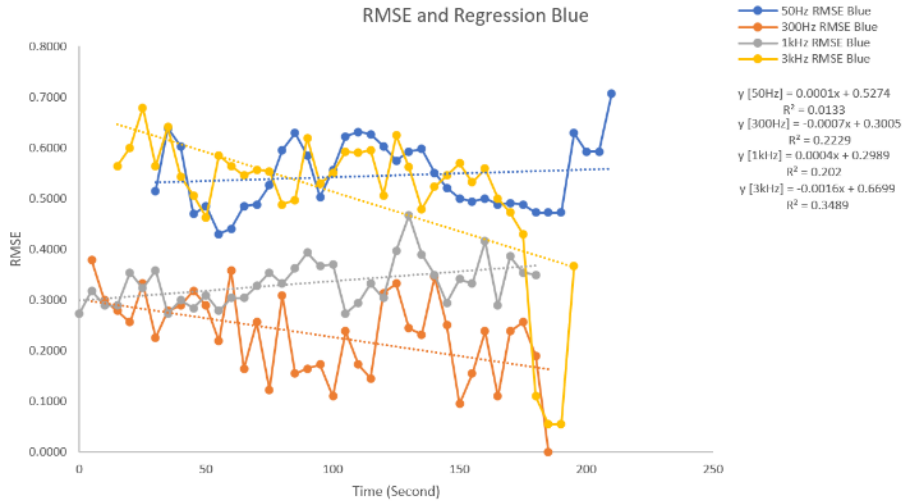

Figure 7. Root means square error and regression R^2 blue

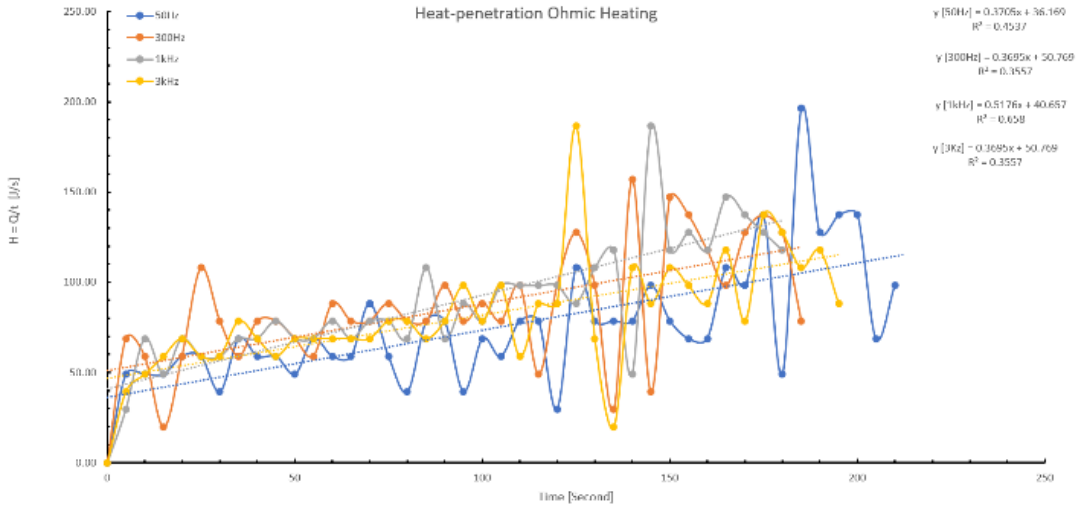

Figure 8. Analysis of chamber heat penetration ohmic heating with regression R^2

Table 4. Quantitative average comparison performance in heat penetration and ohmic heating and efficiency energy validation. The best performances are in red colors.

Frequency	Time (second)	Power Input (Watt)	Heat Penetration Ohmic Heating (Joule/ Second)	Efficiency Energy
50Hz	210	196.36	75.31	38.35%
300Hz	185	185.45	85.2	43%
1kHz	180	268.28	87.52	32.62%
3kHz	195	537.61	80.96	15.05%

Figure 8 illustrates heat penetration using the ohmic heating method. Constant values obtained from the experiment—0.3705 at 50 Hz, 0.3695 at 300 Hz, 0.5176 at 1 kHz, and 0.3695 at 3 kHz—were observed every 5 seconds. The regression (R^2) values were 0.4537 at 50 Hz, 0.3557 at 300 Hz, 0.658 at 1 kHz, and 0.3557 at 3 kHz. These constant values indicate that heat penetration at 1 kHz is remarkably stable during the chamber heat penetration process using the ohmic heating method, as demonstrated in Figure 8. Efficiency, defined as the reduction of energy consumption to achieve the same result, was calculated to determine the percentage of energy saved through the ohmic heating process.

A comparison between power input and heat penetration using the ohmic heating method is detailed in Table 4. The efficiency energy value of 43% at 300 Hz frequency indicates higher efficiency compared to other frequencies. However, the heat penetration ohmic heating value of 87.52% at 1 kHz frequency highlights that heat penetration and efficiency energy are distinct outcomes. The study focuses on the result of heat penetration in ohmic heating for honey processing in a chamber, which is aimed at mass production in the industry.

Conclusions

The study demonstrates that the computer vision domain within food engineering can achieve optimal performance. By comparing various frequencies and validating RMSE values for RGB, as well as Regression R^2, the study selects a frequency of 1 kHz based on the following metrics: RMSE Red at 1.4902, RMSE Green at 0.7017, RMSE Blue at 0.3328, Regression Red at 0.0792, Regression Green at 0.5782, Regression Blue at 0.202, and heat penetration Regression at 0.658. These findings provide a foundation for developing a non-destructive technique that enhances mass production efficiency and time management. Consequently, this paves the way for the advancement of automated ohmic heating systems for honey grading.

Declarations

Conflict of interests The authors declare no competing interests.

References

Alkanan, Z. T., Altemimi, A. B., Al-Hilphy, A. R. S., Watson, D. G., and Pratap-Singh, A. (2021) 'Ohmic heating in the food industry: Developments in concepts and applications during 2013–2020', *Applied Sciences*, 11(6), pp. 1-19

Bhanu, B., and Peng, J. (2000) 'Adaptive integrated image segmentation and object recognition', *IEEE Transactions on Systems, Man and Cybernetics Part C: Applications and Reviews*, 30(4), pp. 427-441

Dhanachandra, N., Manglem, K., and Chanu, Y. J. (2015) 'Image segmentation using k-means clustering algorithm and subtractive clustering algorithm', *Procedia Computer Science*, 54, pp. 764–771

Evahelda, Setiawan, I., Aini, S. N., and Afriani, Z. L. (2021) 'Chemical characteristics of kelulut honey (*Trigona Sp.)* in Bangka Tengah District, Indonesia', *IOP Conference Series: Earth and Environmental Science*, 694(1), pp. 1-7

Hendrawan, Y., and Al Riza, D. F. (2016) 'Machine vision optimization using nature inspired algorithms to model sunagoke moss water status', *International Journal on Advanced Science Engineering and Information Technology*', 6(1), pp. 45–57

Hendrawan, Y., and Murase, H. (2011a) 'Bio-inspired feature selection to select informative image features for determining water content of cultured sunagoke moss', *Expert Systems with Applications*, 38(11), pp. 14321–14335

Hendrawan, Y., and Murase, H. (2011b) 'Neural intelligent water drops algorithm to select relevant textural features for developing precision irrigation system using machine vision', *Computers and Electronics in Agriculture*, 77(2), pp. 214–228

Hu, H., Liu, J., Zhang, X., and Fang, M. (2023) 'An effective and adaptable k-means algorithm for big data cluster analysis', *Pattern Recognition*, 139, pp. 1-18

Javidan, S. M., Banakar, A., Vakilian, K. A., and Ampatzidis, Y. (2023) 'Diagnosis of grape leaf diseases using automatic k-means clustering and machine learning', *Smart Agricultural Technology*, 3, pp. 1-14

Kaur, R., and Kaur, P. (2018) 'Improvement in k-means clustering using varient techniques', 5(9), pp. 359–362

Kumar, A., and Tiwari, A. (2019) 'A comparative study of otsu thresholding and k-means algorithm of image segmentation', *International Journal of Engineering and Technical* Research, 9(5), pp. 12–14

Makroo, H. A., Rastogi, N. K., and Srivastava, B. (2020) 'Ohmic heating assisted inactivation of enzymes and microorganisms in foods: A review', *Trends in Food Science & Technology*, 97, pp. 451–465

Patidar, A. K., Agrawal, J., and Mishra, N. (2012) 'Analysis of different similarity measure functions and their impacts on shared nearest neighbor clustering approach', *International Journal of Computer Applications*, 40(16), pp. 1–5

Park, S. H., Balasubramaniam, V. M., Sastry, S. K., and Lee, J. (2013) 'Pressure-ohmic-thermal sterilization: A feasible approach for the inactivation of bacillus amyloliquefaciens and geobacillus stearothermophilus spores', *Innovative Food Science and Emerging Technologies* 19, pp. 115–123

Patel, K. K., Kar, A., Jha, S. N., and Khan, M. A. (2012) 'Machine vision system: A tool for quality inspection of food and agricultural products', *Journal of Food Science and Technology*, 49(2), pp. 123–141

Patrício, D. I., and Rieder, R. (2018) 'Computer vision and artificial intelligence in precision agriculture for grain crops: A systematic review', *Computers and Electronics in Agriculture*, 153, pp. 69–81

Philipp, I., and Rath, T. (2002) 'Improving plant discrimination in image processing by use of different colour space transformations', *Computers and Electronics in Agriculture*, 35(1), pp. 1–15

Prakash, S. R., and Singh, P. N. (2023) 'Background region based face orientation prediction through hsv skin color model and k-means clustering', *International Journal of Information Technology*, 15(3), pp. 1275–1288

Shafiee, S., Minaei, S., Moghaddam-Charkari, N., and Barzegar, M. (2014) 'Honey characterization using computer vision system and artificial neural networks', *Food Chemistry*, 159, pp. 143–150

Singh, A., Yadav, A., and Rana, A. (2013) 'K-Means with three different distance metrics', *International Journal of Computer Applications*, 67(10), pp. 13–17

Singh, V., and Misra, A. K. (2017) 'Detection of plant leaf diseases using image segmentation and soft computing techniques', *Information Processing in Agriculture*, 4(1), pp. 41–49

Sofu, M. M., Er, O., Kayacan, M. C., and Cetişli, B. (2016) 'Design of an automatic apple sorting system using machine vision', *Computers and Electronics in Agriculture*, 127, pp. 395–405

Vithu, P., and Moses, J. A. (2016) 'Machine vision system for food grain quality evaluation: A review', *Trends in Food Science and Technology*, 56, pp. 13–20

Xing, L., Zhao, H., Lin, Z., and Chen, B. (2023) 'Mixture correntropy based robust multi-view k-means clustering', *Knowledge-Based Systems*, 26, pp. 1-13